Polymer-dominant drag reduction in turbulent channel flow over a superhydrophobic surface

Linsheng Zhang (张林生) [ID] ; Reyna I. Garcia-Gonzalez [ID] ; Colin R. Crick [ID] ; Henry C.-H. Ng [✉] [ID] ;
Robert J. Poole [ID]

Check for updates

CrossMark

View Online

Export Citation

Polymer-dominant drag reduction in turbulent channel flow over a superhydrophobic surface Ⓕ

View Online　　Export Citation　　CrossMark

Linsheng Zhang (张林生),[1] ⓘD Reyna I. Garcia-Gonzalez,[2] ⓘD Colin R. Crick,[2] ⓘD Henry C.-H. Ng,[1,a] ⓘD
and Robert J. Poole[1] ⓘD

AFFILIATIONS

[1] School of Engineering, University of Liverpool, Liverpool L69 3GH, United Kingdom
[2] School of Engineering and Materials Science, Queen Mary University of London, London E1 4NS, United Kingdom

[a] Author to whom correspondence should be addressed: hchng@liverpool.ac.uk

ABSTRACT

In this study, we focused on the integration of a flexible polymer (polyacrylamide) and a (randomly patterned) superhydrophobic surface in a large-scale turbulent channel flow rig to investigate their combined drag reduction effectiveness. Experimental results indicate that, prior to degradation, polyacrylamide (at a 100-ppm concentration) and superhydrophobic surfaces individually manifest drag reductions of 35% and 7%, respectively. However, when combined, the influence of polymer additives remained consistent, with the introduction of superhydrophobic surfaces yielding negligible differences. A clear predominance was evidenced in our facility looking at realistic pressure for applications, with polymer additives overshadowing the impact of superhydrophobic surfaces.

In the pursuit of an environmentally friendly society, extensive research has been devoted to achieving turbulent drag reduction (DR) through diverse techniques.[1] Notably, polymer additives have garnered continuous attention as an active approach for reducing frictional drag in turbulent flows, since the discovery of this phenomenon in 1948.[2] This method achieves substantial DR for flexible polymers by suppressing turbulent motion through polymer stretching.[2,3] Concurrently, superhydrophobic (SHO) surfaces, characterized by their exceptional water repellency,[4] have emerged over the past two decades as a promising passive DR technique, initially in laminar flows[5] and subsequently in turbulent regimes.[6,7] These surfaces leverage hydrophobic chemistry and nano-/micro-scale roughness to trap air at the liquid–solid interface, effectively mitigating wall frictional forces.[8] The application of such surfaces onto existing smooth walls introduces an overall reduction in drag[9] and an extended slip length.[10]

While both techniques have been extensively explored individually, investigations of their combined DR potential are lacking. Recently, Rajappan and McKinley[11] integrated polymer additives and SHO walls in fully turbulent Taylor–Couette flows, yielding a 50% enhancement in DR compared to each individual method. However, these experiments were confined to a test rig operating essentially at atmospheric pressure. In the current study, we explore the combined DR effects of both the polymer additives and the SHO surface in a

large-scale turbulent channel flow (∼700 l), a more realistic setting for practical fluid transport applications. Here, we carefully consider the time-dependent degradation of polymer solutions and SHO surfaces. This broader investigation aims to contribute to a deeper understanding of the intricate interplay between these two distinct DR strategies within larger-scale flow environments.

The rectangular channel shown in Fig. 1(a) has a total length (l) of 7.45 m, comprised of six stainless steel modules, each measuring 1.2 m, and an additional 0.25 m section with float glass side walls housing the SHO surface. The cross-sectional area has dimensions of 25×298 mm^2 ($2h \times w$), where h is the channel half-height, yielding an aspect ratio of 11.92. The working fluid was recirculated by a Mono type E101 progressive cavity pump, while a return loop was available for pre-mixing polymer solutions or achieving a reduced flow rate. To minimize potential pump-induced pulsations, three pulsation dampers were situated prior to the channel inlet. The temperature and flow rate of the working fluid were monitored by a platinum resistance thermometer (PRT) and a flow meter (Promass Coriolis 60), respectively. Multiple pressure ports were drilled underneath the channel to enable pressure measurement at various distances and specifically across the SHO surface area.

Adhering to the approach detailed in the works of Mehanna et al.[15] and Zhang et al.,[16] SHO surfaces were fabricated by applying
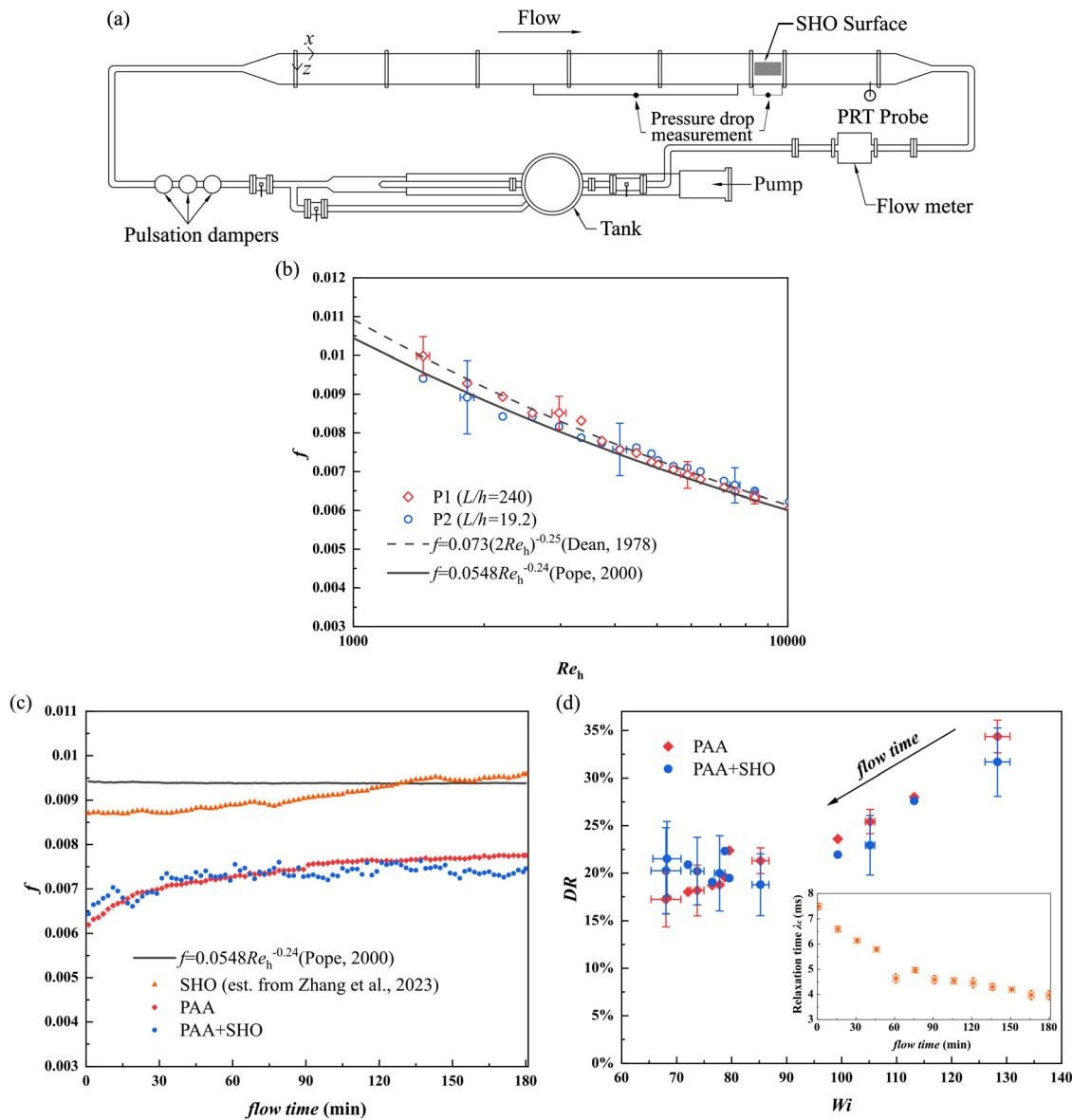
FIG. 1. DR experiments combining polymer additives and SHO surfaces in a turbulent channel flow. (a) Schematic of the channel flow facility. (b) The synchronous pressure drop measurements are benchmarked against the correlations of Dean[12] and Pope.[13] P1 for a long distance ($L/h = 240$) while P2 for a short distance ($L/h = 19.2$), as demonstrated in Fig. 1(a). (c) Friction factors f against flow time for SHO surface alone (estimated from Zhang et al.[14]), PAA solution alone, and PAA + SHO. Pope's correlation[13] is employed as a baseline and plotted in (c). (d) DR against Weissenberg number (Wi) for PAA and PAA + SHO. The relaxation time against flow time is plotted as an inset in (d).

the so-called SPNC (superhydrophobic polymer–nanoparticle composite) material onto a PVC substrate measuring $200 \times 100 \, mm^2$. The coating process comprised two major steps: (1) application of a pre-coating adhesive layer for the PDMS (polydimethylsiloxane) solution and (2) deposition of the PDMS/silica mixture (see Zhang et al.[14]). The coated SHO plate was flush mounted on the bottom wall of the channel and great care was taken to ensure the flatness to better than $\pm 10 \, \mu m$ (see the supplementary material in Zhang et al.[14]). As shown in Fig. 1(a), two pressure ports upstream of the SHO-coated area were

employed to measure pressure drop with polymer solutions exclusively, while an additional two pressure ports across the SHO area were used to measure pressure drop with polymer solutions and the SHO surface concurrently. The synchronous operation of two pressure transducers (P1, Validyne DP14 and P2, Druck LPX-9381) facilitated the acquisition of pressure drop readings as the fluids traversed the channel, thereby ensuring consistency in flow conditions (with consistent flow rate, physical and rheological properties of the fluids). At a constant pump speed, the DR experiments spanned a 3-h duration.

Pressure drop signals were continuously gathered at a data rate of 1000 Hz, and a "local" mean pressure drop ($\overline{\Delta P}$) was calculated on a minute-by-minute basis. The mean wall shear stress ($\overline{\tau_w} = \overline{\Delta P}wh/(l(w+2h))$) was used to calculate the friction factor ($f = \overline{\tau_w}/0.5\rho U_b^2$), wherein ρ denotes the density of the working fluids, and U_b is the bulk velocity (determined by the flow rate).

Polyacrylamide (PAA), possessing a molecular weight of approximately 22×10^6 g/mol,[17] was dissolved in tap water to prepare the polymer solution at a nominal concentration of 100 ppm. In anticipation of degradation in PAA[18] solution under shear, fluid samples were collected every 15 min of flow time for shear and extensional rheological characterization, conducted using an Anton Paar MCR302 shear rheometer and a HAAKE™ CaBER1 capillary beak-up extensional rheometer, respectively. Therefore, changes in shear viscosity and relaxation time of the PAA solution were closely tracked over the course of the flow measurements. The measured viscosity curve from the rheometer established a link between shear rate and shear stress, enabling the estimation of the "true" viscosity of the PAA solution during channel flow experiments. In addition to alterations in fluid properties, we further characterized the interaction between PAA and SPNC surfaces through contact angle measurements. As displayed in Table I, the contact and sliding angles for water, PAA, and degraded PAA remain constant. This suggests that under no-flow conditions, a non-wet SPNC surface can be sustained regardless of the degradation of PAA solutions. In addition, the surface tension of PAA solutions was also confirmed to be equal with water ($\sim$72.6 mN/m), using the Wilhelmy plate method (via a Kruss K100 surface tensiometer). A laminar-flow slip length measurement[16] was conducted to investigate the possibility of polymer adsorption by the SHO surface. The results suggest that there is minimal evidence of polymer molecules being adsorbed by the surface since the slip length with PAA ($\sim$100 μm) is slightly greater than with water ($\sim$93 μm).

Benchmark Newtonian friction factor (f) profiles (against Dean[12] and Pope[13]) of the channel flow facility, utilizing two transducers, were established prior to conducting DR experiments. The two transducers measure pressure drop over distinct sections of the channel with water under classical no-slip boundary conditions. Figure 1(b) displays the friction factor plotted against various Reynolds numbers ($Re_h = \rho U_b h/\mu$), where μ is the viscosity. The data exhibit a favorable agreement with both $f = 0.073(2Re_h)^{-0.25}$ (Dean's correlation[12]) and $f = 0.0548Re_h^{-0.24}$ (Pope's correlation[13]) within the high Reynolds number regime. However, a better agreement was observed with $f = 0.0548Re_h^{-0.24}$ for $1000 < Re_h < 2000$. In order to sustain an extended air plastron over SHO surfaces, a comparatively lower Reynolds number ($\sim$1500) was selected for the following DR tests. This Reynolds number offers sufficient turbulence to stretch the

TABLE I. Superhydrophobicity characterization of SPNC surfaces with various liquids.

Liquids	Tap water	PAA[a]	PAA-degraded[b]
Contact angle (°)	153.4 ± 3.4	151.8 ± 2.3	152.3 ± 0.4
Sliding angle (°)	3.2 ± 1.2	3.4 ± 1.8	3.6 ± 1.0

[a]PAA solution at a nominal concentration of 100 ppm.
[b]This degraded PAA sample was collected at the end of the DR experiment (at 180 min) when its elasticity (relaxation time) dropped to a constant.

polymer molecules and is free of transitional effects,[19] thus facilitating DR (i.e., the characteristic timescale of the flow is comparable to the relaxation time of the polymer solution[18]) as evidenced by preliminary tests utilizing only polymer solutions.

Time-dependent pressure drop measurements were conducted within the channel, incorporating both polymer solutions (PAA) and SHO surfaces. As depicted in Fig. 1(c), the friction factors calculated from two synchronized pressure drop results (representing measurements with PAA alone and both PAA + SHO) were plotted against flow time. The data for SHO only were extrapolated from a recent study involving a closely related Reynolds number (approximately 1700).[14] Furthermore, Pope's correlation[13] was utilized as a baseline due to its superior alignment within the low Reynolds number range, as depicted in Fig. 1(b). Evidently, when utilizing only SHO surfaces, the friction factor (f) increases over time and converges toward the no-slip line (Pope's correlation[13]) by the end of the test. This is emphasized by the DR capacity of SHO surfaces diminishing over time due to the progressive loss of the air plastron. The gauge pressure over the SHO surface during the experiment was measured at 4.3 kPa. This pressure allows the surface to provide a certain degree of DR for a specific duration, as reported in Zhang et al.[14] The peak DR achieved by the SHO surface is approximately 7%, and this peak is sustained for 30 min. Owing to the shear-induced degradation of PAA, f with PAA alone exhibited an initial increase. The degradation of PAA was characterized through CaBER measurements, with results illustrated as an inset in Fig. 1(d) (the relaxation time λ_c against flow time). Notably, in comparison with SHO surfaces, f remained considerably lower over the entire duration when using PAA alone, demonstrating its significantly greater DR potential. The friction factor stabilizes to a constant value at the end of the test (i.e., 180 min) yet still yields a notable 17% DR based on calculations derived from Pope's correlation. Friction factors for PAA + SHO showed no obvious distinction from PAA alone considering the experimental uncertainties.

We noticed that the synergistic DR effect, reported by Rajappan and McKinley[11] in turbulent Taylor–Couette (T–C) flow, has not been replicated in the current channel flow setup. According to the velocity measurements presented in Zhang et al.,[14] the slip length over the current SHO surface reached a maximum of $\sim$62.5 μm, occurring at a relatively low Reynolds number ($Re = 1500$). This value corresponds to an inner-scale slip length b^+ of 0.45 in the current study. Moreover, the DR achieved by PAA was approximately five times greater than that of the SHO surface in the initial stages of the experiment and this difference became increasingly significant while the surface degraded with flow time. Therefore, it is perhaps not surprising that with this relatively small b^+ value, the surface does not produce appreciable DR in comparison to the rather significant DR effect induced by the polymer additives. Note that the T–C flow setup of Rajappan and McKinley[11] operated at essentially atmospheric pressure, thus, much higher Reynolds numbers ($Re_\tau = 800$–2000) were reached and consequently, their inner-scaled slip length (b^+) would be significantly larger than we have achieved here, despite the possibility that the dimensional slip lengths generated by their SHO surfaces may be similar with ours. Therefore, it is reasonable to assume that the contribution of SHO surfaces to the overall DR in their study is greater compared to our setup. We also note that Rajappan and McKinley's combined DR of 27% was not a simple linear addition of the two components (each being 18%): if this reduction was all due to a reduction in the

drag-reduction effectiveness of the SHO surface (i.e., by 50%), then, as our SHO individual DR is just 7% at early times, a 50% reduction would put us within the uncertainty of our measurements. Thus, our results are potentially not inconsistent with those of Rajappan and McKinley.[11]

In our specific scenario, to observe a notable contribution from the SHO surface, we estimate that SHO surfaces might need to independently generate at least a 17% drag reduction. This level of drag reduction is equivalent to the effect induced by the PAA additives at their minimum effectiveness. Therefore, given a fixed $b = 62.5\,\mu$m (as reported in Zhang et al.[14]), achieving a significantly higher Reynolds number would be necessary to obtain the DR $= 17$% solely by SHO surfaces. However, in the context of high Reynolds numbers and a channel rig like the one presented in this study, the elevated absolute pressure over the surface can instantly remove the air plastron, resulting in little to no drag reduction effect. The dilemma in a large-scale channel flow is essentially that, at low Reynolds numbers, you can maintain the plastron (as the static pressure on the working section remains low) but the effect of the slip is only small (as can be estimated by calculating this length in "inner" units). At higher Reynolds numbers, where at fixed dimensional slip length the slip length now becomes more significant in inner units, the pressure is high such that the plastron cannot be maintained.

Additionally, polymer-induced DR was not affected by a slip boundary condition since the friction factor curves overlapped the whole time whether an air layer existed or not. Figure 1(d) illustrates DR from both PAA alone and PAA + SHO plotted against Weissenberg number ($Wi = U_b \lambda_c / h$). In both cases, DR diminishes over time, reaching an apparent steady state, and exhibits a discernible correlation with Wi, which is in good agreement with the previous work on polymer DR alone.[18] This indicates that the polymer stretching plays a dominant role in reducing turbulent frictional drag in the current setup and obscures the impact of the SHO surface.

As representatives for both active[20,21] and passive control[22] techniques of turbulent flow, the effectiveness of incorporating polymer additives and SHO surfaces has been investigated. A flexible polymer (polyacrylamide) and a randomly patterned SHO surface (SPNC), both in widespread use in DR research, were utilized in a large channel flow facility to achieve turbulent DR. Our results indicate that the synergistic effect arising from combining polymer additives and SHO surfaces, reported in a small-scale T–C setup,[11] is not easily reproduced in a large-scale flow rig closer to real-world fluid transport application. Instead, polymer additives emerge as the predominating factor in this context, overshadowing the potential contributions of the SHO surfaces, at least in the current setup, which operates at the significantly higher gauge pressure (~ 4 kPa). It is worth pointing out that polymer solutions can still maintain their ability to produce DR when a slip wall is involved. We anticipate the relatively small b^+ value might not have a major impact on the primary flow turbulence. Consequently, the functionality of polymer additives remains consistent irrespective of the different wall conditions.

AUTHOR DECLARATIONS
Conflict of Interest

The authors have no conflicts to disclose.

Author Contributions

Linsheng Zhang: Data curation (lead); Methodology (equal); Software (lead); Visualization (lead); Writing – original draft (lead). **Reyna Itzel Garcia-Gonzalez:** Resources (supporting). **Colin R. Crick:** Resources (equal); Supervision (supporting); Writing – review & editing (equal). **Henry C. H. Ng:** Methodology (equal); Software (supporting); Supervision (supporting); Writing – review & editing (equal). **Robert John Poole:** Conceptualization (lead); Methodology (equal); Resources (equal); Supervision (lead); Writing – review & editing (equal).

DATA AVAILABILITY

The data that support the findings of this study are available from the corresponding author upon reasonable request.

REFERENCES

[1] S. Ghaemi, "Passive and active control of turbulent flows," Phys. Fluids **32**, 080401 (2020).

[2] L. Xi, "Turbulent drag reduction by polymer additives: Fundamentals and recent advances," Phys. Fluids **31**, 121302 (2019).

[3] C. M. White and M. G. Mungal, "Mechanics and prediction of turbulent drag reduction with polymer additives," Annu. Rev. Fluid Mech. **40**, 235–256 (2008).

[4] H. Wang, H. Lu, and W. Zhao, "A review of droplet bouncing behaviors on superhydrophobic surfaces: Theory, methods, and applications," Phys. Fluids **35**, 021301 (2023).

[5] C. Lee, C.-H. Choi, and C.-J. Kim, "Superhydrophobic drag reduction in laminar flows: A critical review," Exp. Fluids **57**, 1–20 (2016).

[6] W. Abu Rowin, J. Hou, and S. Ghaemi, "Inner and outer layer turbulence over a superhydrophobic surface with low roughness level at low Reynolds number," Phys. Fluids **29**, 095106 (2017).

[7] W. Abu Rowin and S. Ghaemi, "Effect of Reynolds number on turbulent channel flow over a superhydrophobic surface," Phys. Fluids **32**, 075105 (2020).

[8] J. P. Rothstein, "Slip on superhydrophobic surfaces," Annu. Rev. Fluid Mech. **42**, 89–109 (2010).

[9] R. J. Daniello, N. E. Waterhouse, and J. P. Rothstein, "Drag reduction in turbulent flows over superhydrophobic surfaces," Phys. Fluids **21**, 085103 (2009).

[10] C.-H. Choi and C.-J. Kim, "Large slip of aqueous liquid flow over a nanoengineered superhydrophobic surface," Phys. Rev. Lett. **96**, 066001 (2006).

[11] A. Rajappan and G. H. McKinley, "Cooperative drag reduction in turbulent flows using polymer additives and superhydrophobic walls," Phys. Rev. Fluids **5**, 114601 (2020).

[12] R. B. Dean, "Reynolds number dependence of skin friction and other bulk flow variables in two-dimensional rectangular duct flow," J. Fluid Eng. **100**, 215–223 (1978).

[13] S. B. Pope, *Turbulent Flows* (Cambridge University Press, 2000).

[14] L. Zhang, C. R. Crick, and R. J. Poole, "*In situ* monitor of superhydrophobic surface degradation to predict its drag reduction in turbulent flow," Appl. Phys. Lett. **123**, 064101 (2023).

[15] Y. A. Mehanna and C. R. Crick, "Image analysis methodology for a quantitative evaluation of coating abrasion resistance," Appl. Mater. Today **25**, 101203 (2021).

[16] L. Zhang, Y. A. Mehanna, C. R. Crick, and R. J. Poole, "Surface tension and viscosity dependence of slip length over irregularly structured superhydrophobic surfaces," Langmuir **38**, 11873–11881 (2022).

[17]V. C. Ibezim, R. J. Poole, and D. J. Dennis, "Viscoelastic fluid flow in microporous media," J. Non-Newtonian Fluid Mech. **296**, 104638 (2021).

[18]B. E. Owolabi, D. J. Dennis, and R. J. Poole, "Turbulent drag reduction by polymer additives in parallel-shear flows," J. Fluid Mech. **827**, R4 (2017).

[19]R. Agrawal, H. C.-H. Ng, D. J. Dennis, and R. J. Poole, "Investigating channel flow using wall shear stress signals at transitional Reynolds numbers," Int. J. Heat Fluid Flow **82**, 108525 (2020).

[20]B. Lin, H.-B. Hu, L. Jiang, Z. Li, and L. Xie, "Development and drag-reducing performance of a water-soluble polymer coating," Phys. Fluids **35**, 063120 (2023).

[21]L. F. Mortimer and M. Fairweather, "Prediction of polymer extension, drag reduction, and vortex interaction in direct numerical simulation of turbulent channel flows," Phys. Fluids **34**, 073318 (2022).

[22]J. Hu and Z. Yao, "Drag reduction of turbulent boundary layer over sawtooth riblet surface with superhydrophobic coat," Phys. Fluids **35**, 015104 (2023).

08 January 2024 10:10:44